Advanced Geo-Data Analytics and AI for 3D Flood Mapping to Protect Built Assets

[1] Jeffrey Blay, [2] Leila Hashemi-Beni

College of Science and Technology, North Carolina A&T State University, 1601 E Market St, Greensboro, NC-USA
[1] jblay@aggies.ncat.edu, [2] lhashemibeni@ncat.edu

Keywords: Flood Depth, Remote Sensing, Deep Learning, Impact Assessment, Natural Disaster.

Abstract

Floods are among the most destructive natural disasters, posing significant risks to human lives and property. This study investigates the impact of Hurricane Matthew on built assets in Greenville, North Carolina, USA in 2016 using an integrated approach that combined floodwater extent mapping, depth estimation, and impact assessment. In particular, our objective is to accurately map and estimate floodwater depth using deep learning techniques combined with aerial imagery and lidar data to assess the extent of flooding's impact on critical infrastructure such as buildings and roads. The pretrained UNET model utilized, achieved high accuracy in mapping flood extent, with a 93% accuracy, while floodwater depth estimates yielded a root mean square error (RMSE) of 0.75, reflecting a deviation of approximately 1ft from field measurements. The results highlighted the severe damage sustained by essential assets, notably Greenville Airport, which experienced significant flooding and disruption. The research results revealed that approximately 32% (415 acres) of developed land, 26% (185) of buildings, and 66% (23 miles) of roads were affected. These findings provide critical insights that can guide policymakers in crafting effective mitigation and adaptation strategies to protect urban areas and essential infrastructure.

1. Introduction

The increasing frequency and intensity of climate change-driven flooding poses a growing threat to lives and properties, particularly in flood-prone areas. Globally, projections indicate that by 2100, 52% of the population and 46% of all assets will be at risk from intensified flooding. Also, the frequency of flood will continue to rise, with areas near rivers likely to experience flooding every 10-50 years, instead of the anticipated 100 year interval (Wienhold et al., 2023). In the United States, flooding from major tropical cyclones has consistently inflicted severe economic damage, especially in urban and coastal areas. Hurricanes like Harvey (2017) and Ian (2022) caused over USD 100 billion in economic losses combined, while earlier storms, such as Katrina (2005), was responsible for more than USD 5 billion in infrastructural damage across Alabama, Louisiana, and Mississippi (Museru et al., 2024; Shahabi and Tahvildari, 2024). These extensive societal and financial damages can be attributed to the fact that over 80% of the population in the United States are located in urban areas (World Bank, 2023).

Coastal states are particularly vulnerable to these devastating flood events. Studies predict that by 2100, the area to U.S. coastal floodplains susceptible to a 100-year flood event could expand by 55% if shorelines remain fixed (Alizadeh Kharazi and Behzadan, 2021). North Carolina, for example, suffered catastrophic damage from Hurricane Matthew in 2016. Reports from local, state, and federal agencies estimated economic losses of about USD 5 billion, including the destruction of roughly 110,000 homes and businesses, as well as severe impacts to electricity infrastructure, with inundated substations and blown transformers, leaving approximately 900,000 people without electricity (Benfield, 2017; Berg, 2017). Given the increasing severity, frequency, and impact of flooding, there is a pressing need to leverage advanced technology to map and assess risks and vulnerabilities in populated areas, helping to mitigate future losses.

Access to accurate and timely information following major natural disasters, such as floods, is crucial for effective emergency response and recovery. Additionally, it plays a vital role in supporting mitigation and adaptation strategies aimed at ensuring long-term socio-economic and environmental resilience in vulnerable areas. (Alizadeh Kharazi and Behzadan, 2021).

Consequently, researchers have increasingly applied advanced remote sensing techniques to efficiently map and analyze flood dynamics (Do Lago et al., 2023; Gebrehiwot and Hashemi-Beni, 2021). Other studies have focused on flood damage and susceptibility mapping (Museru et al., 2024; Wang et al., 2020). Moderate resolution satellite imagery, including Landsat 8 and Sentinel 2 provide valuable information for mapping flooded areas, as well as training models for predicting flood vulnerabilities and damage assessment for various flood scenarios. Additionally, other remotely sensed datasets, including radar imagery (e.g. Sentinel 1, PALSAR-2) (Cian et al., 2018; Iervolino et al., 2015; Schumann et al., 2007), aerial imagery (including UAV imagery) (Fonstad and Marcus, 2005; Scorzini et al., 2018), as well as surveillance camera footage(e.g. river cameras) (Liu and Huang, 2024; Moy De Vitry et al., 2019) have been relied on for various flood studies.

Traditionally, classical remote sensing methods and machine learning techniques were applied to process and extract meaningful environmental information from these datasets for different applications (Agboola and Hashemi-Beni, 2023; Anokye et al., 2024; Wasehun et al., 2024) ; However, these methods tend to yield low accuracy results due to the complex textual information and nonlinear relationships between flood related variables, especially in complex environments like the urban area (Gebrehiwot and Hashemi-Beni, 2022). The use of advanced deep learning networks, particularly convolutional neural networks (CNNs), for flood mapping and assessment is increasingly being adopted to address existing limitations and demonstrate high performance (Gebrehiwot et al., 2019; Hashemi-Beni et al., 2024). CNNs excel at learning and detecting complex nonlinear relationships among features through various convolutional operations.

Their capability to process and extract information from raw image data, leveraging spatial information at the pixel level, has contributed to their widespread acceptance and application within the remote sensing community. (Guo et al., 2020; Hashemi-Beni and Gebrehiwot, 2021). Various remote sensing studies have applied different CNN network architectures for flood mapping, with the UNET architecture being particularly prevalent in studying various flood dynamics (Kabir et al., 2023; Popandopulo et al., 2023; Yokoya et al., 2022). Other architectures, such as Mask R-CNN (Alizadeh Kharazi and

Behzadan, 2021; Song and Tuo, 2021), conditional Generative Adversarial Network (cGAN) (Burrichter et al., 2023; Do Lago et al., 2023), and Deeplabv3+ (Muhadi et al., 2024) have also been applied for similar purposes. Despite its robust capabilities, deep learning is inherently data-intensive, requiring sufficient high-quality data to achieve optimal performance.

Rarely do studies provide a comprehensive approach that includes floodwater extent mapping, water depth estimation, and impact assessment. This study aims to address this limitation by leveraging artificial intelligence and advanced remote sensing techniques to predict floodwater extent, estimate water depth, assess the impact on building structures and road infrastructure in settlement areas. This integrated analysis offers a comprehensive perspective on flood dynamics and potential impacts, with each indicator contributing valuable insights essential for shaping sustainable flood mitigation and adaptation policies.

2. Data and Methodology

2.1 Study Area

The study focused on Greenville, a city in Pitt County, North Carolina, USA. Situated in the north-central coastal plains region of East North Carolina, Greenville was significantly impacted by Hurricane Matthew, which brought severe flooding to the coastal plains, causing widespread damage to both lives and properties.

Our analysis focused on the Greenville airport enclave (Figure 1), with a land cover area of 1,981 acres. The area constitutes approximately 66% built-up areas, 19% open water, 15% vegetation, and less than 1% other land cover types (Figure 2). This area includes around 708 buildings and approximately 35 miles of roadway (Table 1).
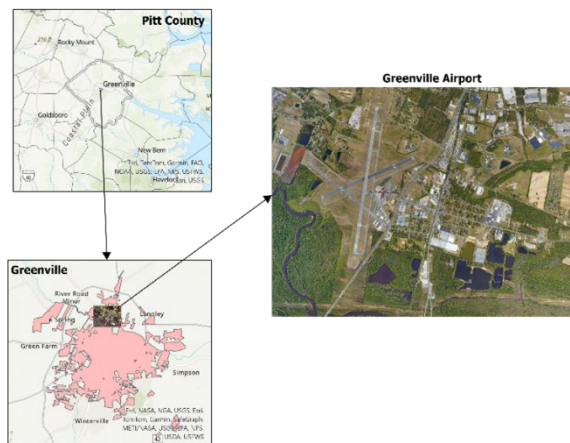

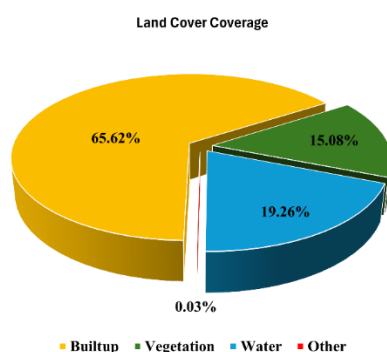Figure 1: Study area map of Greenville airport enclave

Figure 2: Landcover types for study area

Built assets	Total
Building structures	708
Roads	34.94 miles

Table 1: Building structures and road infrastructure statistics.

2.2 Data

To achieve the study objective, a range of geospatial datasets were employed. The primary data sources included post-flood aerial imagery from NOAA, landcover data from the National Land Cover Database (NLCD), lidar data and building footprints from North Carolina Emergency Management (NCEM), and road data from Open Street Map (OSM) (Figure 2).

The post flood aerial imagery, with a resolution of approximately 25 cm was downloaded from the NOAA web portal and used for mapping flooded areas within the study area. The 2016 Land Cover dataset for the Continental United States (CONUS) was accessed from the NLCD web portal, at a resolution of approximately 30 m, was employed to estimate land cover types in the study area. Lidar data, derived from the North Carolina Spatial data web portal, at 2 points per meter resolution for 2015, was used to generate a digital elevation (DEM) raster for the study area. Building footprints for 2020 were accessed from the same source. Additionally, road data was extracted from open street map (osm) using a plugin API in QGIS. These datasets facilitated the impact assessment analysis. USGS field measurements of floodwater depth was also utilized as reference points for evaluating the accuracy of the floodwater depth estimates.
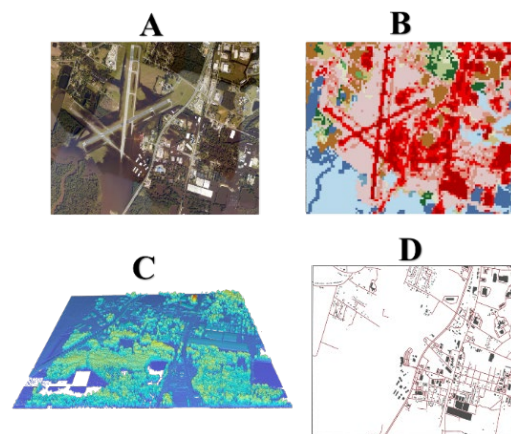

Figure 3: (A) Post flood Aerial imagery. (B) National landcover data. (C) Lidar data from NCEM. (D) Building footprint, and road data (osm).

2.3 Methodology

The methodology leveraged the artificial intelligence (AI) capabilities of ArcGIS pro, combined with a series of key steps to delineate floodwater extent, and estimate floodwater depth. This approach facilitated a detailed analysis of flood impact on building structures and road infrastructure within the designated study area. The flowchart (Figure 4) shows the steps of the proposed methodology, which are further outlined below :
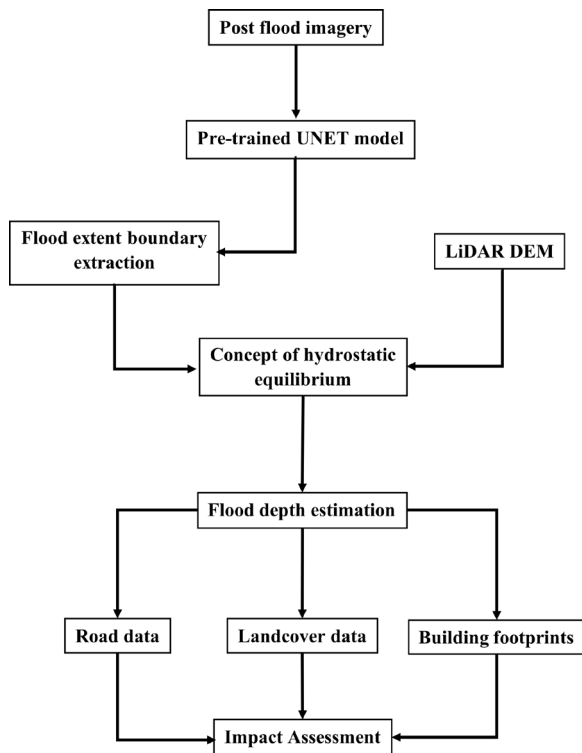
Figure 4: Flowchart of the proposed methodology

2.3.1 Floodwater Extent Boundary Extraction: To estimate floodwater depth, identifying flooded areas within the study region is essential. The initial step in our methodology focused on delineating these areas using the post-flood aerial imagery, which is processed through the UNET image segmentation algorithm. The UNET model, originally proposed by (Ronneberger et al., 2015), is highly effective for image segmentation tasks and is widely recognized for its performance in similar applications (Blay et al., 2024; Guo et al., 2022; Kabir et al., 2023).

The UNET architecture is a U-shaped network, constituting two main parts; a contracting path for downsampling and an expansive path for upsampling. The contracting path applies 3x3 convolutions with ReLU and 2x2 max-pooling, doubling the feature channels at each step. The expansive path upsamples with 2x2 convolutions, concatenates with cropped feature maps from the contracting path, and uses additional two 3x3 convolutions, each followed by a ReLU activation to refine results. The final layer map features to classes with a 1x1 convolution, amounting to a total of 23 convolutional layers. Furthermore Input tile sizes are chosen to ensure smooth tiling of the segmentation output (Ronneberger et al., 2015).

For this study, we leveraged a pre-trained UNET model, specifically the "High resolution Land Cover Classification-USA" model available in the ArcGIS python API. This model, trained on the Chesapeake Bay Landcover dataset, has an overall accuracy of approximately 87%, and about 93% in precision, recall, and F1-score for detecting open water areas (ESRI, 2024). The UNet model was employed to perform segmentation of the post flood aerial imagery into seven (7) land cover classes. Our primary interest was in the open water class, so we extracted the water class and qualitatively reviewed it for any misclassifications, including errors of commissions or omissions in this category. Any misclassifications, such as the classification of other land cover classes as open water, or otherwise, were corrected (Figure 5).

The following steps summarize ArcGIS Pro deep learning implementation workflow;

1. Segmentation of Imagery: Loaded the post-flood aerial imagery into the 'Classify Pixels using Deep Learning' tool, and segment it into seven land cover classes using the pre-trained model. Converted segmented raster results into polygon using "Raster to Polygon" tool.

2. Visual Quality Assessment (VQA): Conducted a post-segmentation VQA focused on the open water class and other landcover types (Figure 6).

3. Extraction of Flooded Areas: Used SQL Query Builder to extract the open water class, from the segmentation results, as an indicator for flooded areas.

4. Flood Extent Assessment: Refine the floodwater extent delineation and finalize results.

This workflow enabled efficient segmentation and extraction of floodwater extent, leveraging artificial intelligence capabilities to accurately identify open water areas (Figure 5 and 6).
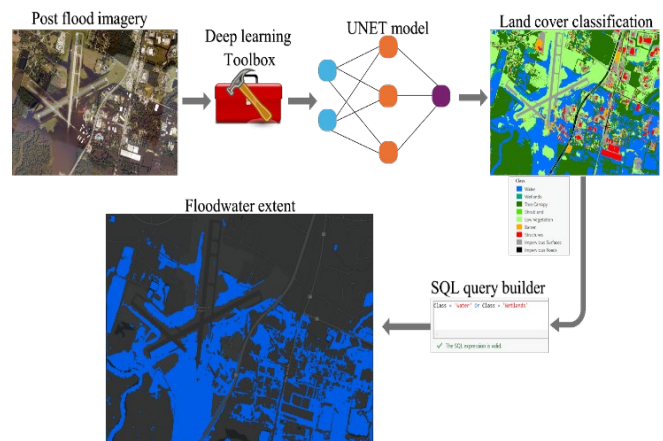

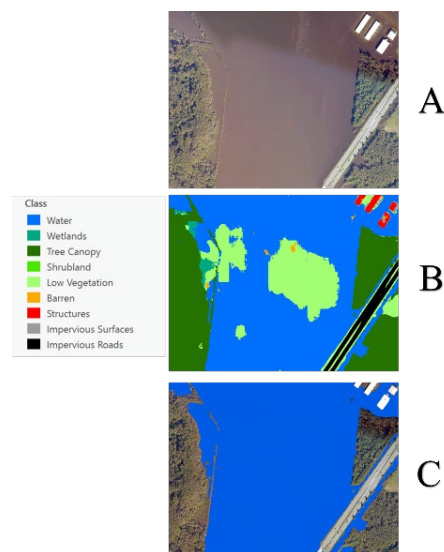
Figure 5: Floodwater extent delineation workflow.

Figure 6: (A) aerial imagery. (B) segmentation results with water misclassification. (C) Final floodwater extent post VQA

2.3.2   Floodwater depth estimation and Impact assessment:
Our approach for estimating the floodwater depth is based on a knowledge-based approach employed by various studies (Blay et al., 2024; Gebrehiwot and Hashemi-Beni, 2021; Surampudi and Kumar, 2023; Wienhold et al., 2023), which leverages on just floodwater extent and an underlying DEM data. This approach is a pixel-wise estimation of floodwater depth within a flood domain, by deducting the water surface height from the underlying DEM (Blay et al., 2024). This approach is based on the principle of hydrostatic equilibrium, which states that stationary fluids exert equal pressure in all directions due to gravitational forces. This causes water to flow into lower areas, creating a relatively level surface in the absence of flow. Thus, we can assume that the water surface along the perimeter of the flooded area is close to a uniform elevation. By interpolating this water surface height using the water extent, we can estimate the floodwater depth by subtracting it from the DEM, giving an estimated water level within each flooded region. After obtaining these floodwater depth estimates, we overlaid building and road infrastructure, as well as the landcover data on the flood map to assess the impact, determining the number of affected buildings, roadways, and the extent of affected developed areas within the study area. Our implementation followed the steps outlined in (Blay et al., 2024), allowing for an effective evaluation of flood depth and its impact on built infrastructure.

In summary, the implementation workflow included; (1) Clipping the underlying DEM to the floodwater extent boundary; (2) extracting elevation values along the water extent perimeter from the clipped DEM; (3) using linear interpolation to estimate the water surface heigh for each flooded area; and (4) calculating floodwater depth by subtracting the estimated water surface height from the underlying DEM (Figure 7).
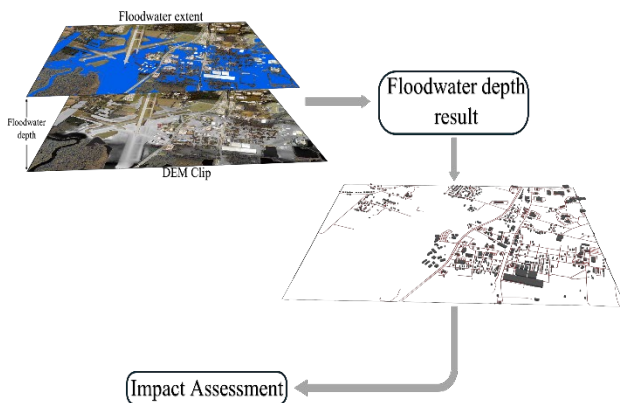

Figure 7: Floodwater depth and impact assessment workflow

3.   Results and Discussion

The estimated floodwater depth results revealed a maximum water depth of approximately 16ft within the Greenville airport enclave. Due to the absence of actual field measurements specific to our study site, field gage height measurement data from USGS on the Tar River was used as a reference for accuracy assessment using the RMSE score. Our floodwater depth achieved an RMSE score of 0.75, indicating an average deviation of approximately 1ft between our water depth estimation and the reference measurement. This deviation may be attributed to several factors, including the temporal mismatch between datasets, the reliability of the ground truth data for the study areas, and minor inaccuracies in both the floodwater extent results and the DEM data.

The flooded areas were concentrated primarily in the southern part of the study area (Figure 8), with the highest depth levels clustered around the south and southwest of the Greenville airport (Figure 9). Given the proximity of these areas to the floodplains of the Tar River, this result aligns with expectations. Further analysis revealed that approximately 32% (about 415 acres) of the total 1300.5 acres of the builtup area within the airport enclave was affected by flooding. Furthermore, approximately 26% (185) of the total building structures and 66% (23 miles) of road infrastructure within the study area were impacted by the hurricane (Figure 10).

As illustrated in Figure 10, critical built assets such as the Greenville airport and various commercial and residential buildings, suffered substantial impacts. This level of damage underscores the potential for significant economic losses to the city following the hurricane. For instance, various state reports revealed that approximately 30,000 businesses across the state suffered physical damage or operational interruptions, with estimated losses totaling USD 2 billion (Benfield, 2017). Additionally, many smaller roads, including those in Greenville, were expected to be closed for months due to the extent of the damage caused by the hurricane. This widespread impact highlights the severe economic and infrastructural challenges incurred by the affected communities, including Greenville.

4.   Conclusion

Comprehensively mapping floodwater extent, estimating the water depth, as well as analyzing the flood impact in populated areas provides in-depth insights into flood dynamics and strategies for mitigating severity. This study leveraged geospatial datasets and artificial intelligence to map floodwater extent, estimate flood water depth and assessed its impact on buildings and roads affected by Hurricane Matthew in Greenville, North Carolina. The deep learning and geospatial analytical capabilities were integrated with aerial imagery, lidar-derived DEM, building and road data, as well as landcover data. Our findings show that Hurricane Matthew affected 32% of developed land, 26% building structures, and approximately 66% of roads within study area. Notable assets, such as the Greenville airport, were significantly affected. Flood extent results achieved 93% accuracy, while floodwater depth estimation showed RMSE of 0.75, indicating a deviation from the ground truth measurements of approximately 1 ft.
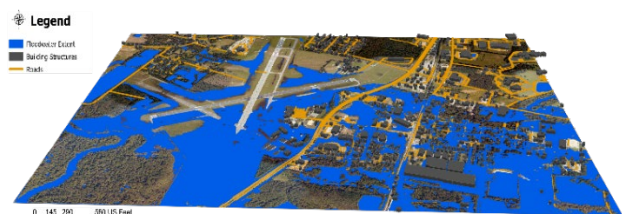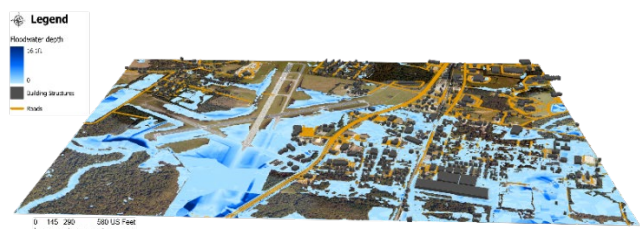

Figure 8: Floodwater extent result

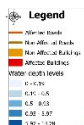Figure 9: Floodwater depth estimation result

Figure 10: Impact assessment results with ground truth

Despite the study's comprehensive approach, several improvements are needed for future research. A key limitation is using DEMs to estimate floodwater depth in complex urban terrains, as it may lead to significant underestimations. DEMs tend to oversimplify urban landscapes, smoothing out critical elevation variations caused by buildings, bridges, roads, artificial slopes, and vegetation—features that influence natural water flow. This simplification can lead to inaccuracies and misclassify high-risk areas. Another key limitation is the temporal mismatch in datasets used, as all were captured at different times. For example, the aerial imagery was captured in 2016, while building footprint data dates to 2020—four years post-disaster. This discrepancy may introduce inaccuracies in the impact assessment, potentially identifying buildings that did not exist at the time of the disaster as affected or overlooking those that were impacted. Future studies should find comprehensive ways of addressing these challenges to improve flood mapping and impact assessment. Such improvements could significantly strengthen emergency response planning and infrastructure resilience initiatives.

Acknowledgements

References

Agboola, A. and Hashemi-Beni, L., "Geospatial Insights: Unraveling Howard Landslide Suspectibility," *IGARSS 2024 - 2024 IEEE International Geoscience and Remote Sensing Symposium*, Athens, Greece, 2024, pp. 3014-3017, doi: 10.1109/IGARSS53475.2024.10641633.

Alizadeh Kharazi, B., Behzadan, A.H., 2021. Flood depth mapping in street photos with image processing and deep neural networks. Computers, Environment and Urban Systems 88, 101628. https://doi.org/10.1016/j.compenvurbsys.2021.101628

Anokye, M., Fawakherji M., and Hashemi-Beni, L., (2024), "Flood Resilience Through Advanced Wetland Prediction," *IGARSS 2024 - 2024 IEEE International Geoscience and Remote Sensing Symposium*, Athens, Greece, 2024, pp. 5516-5520, doi: 10.1109/IGARSS53475.2024.10641585.

Benfield, A., 2017. Hurricane Matthew Event Recap Report.

Berg, R., 2017. Hurricane Matthew.

Blay, J., Fawakherji, M., Hashemi-Beni, L., 2024. Flood impact risk mapping in settlement areas from a 3D perspective: A case study of hurricane matthew. Presented at the 2024 IEEE International Geoscience and Remote Sensing Symposium, IEEE, Athens, Greece. https://doi.org/10.1109/IGARSS53475.2024.10640634.

Burrichter, B., Hofmann, J., Koltermann Da Silva, J., Niemann, A., Quirmbach, M., 2023. A Spatiotemporal Deep Learning Approach for Urban Pluvial Flood Forecasting with Multi-Source Data. Water 15, 1760. https://doi.org/10.3390/w15091760

Cian, F., Marconcini, M., Ceccato, P., 2018. Normalized Difference Flood Index for rapid flood mapping: Taking advantage of EO big data. Remote Sensing of Environment 209, 712–730. https://doi.org/10.1016/j.rse.2018.03.006

Do Lago, C.A.F., Giacomoni, M.H., Bentivoglio, R., Taormina, R., Gomes, M.N., Mendiondo, E.M., 2023. Generalizing rapid flood predictions to unseen urban catchments with conditional generative adversarial networks. Journal of Hydrology 618, 129276. https://doi.org/10.1016/j.jhydrol.2023.129276

Wasehun, E. T., Beni, L. H., Di Vittorio, C. A., Zarzar, C. M., & Young, K. R. (2024). Comparative analysis of Sentinel-2 and PlanetScope imagery for chlorophyll-a prediction using machine learning models. *Ecological Informatics*, 102988.

ESRI, 2024. ArcGIS Pre-trained Models [WWW Document]. introduction-to-high-resolution-land-cover-classification-usa. URL https://doc.arcgis.com/en/pretrained-models/latest/imagery/introduction-to-high-resolution-land-cover-classification-usa.htm (accessed 9.20.24).

Fonstad, M.A., Marcus, W.A., 2005. Remote sensing of stream depths with hydraulically assisted bathymetry (HAB) models. Geomorphology 72, 320–339. https://doi.org/10.1016/j.geomorph.2005.06.005.

Gebrehiwot, Asmamaw, Leila Hashemi-Beni, Gary Thompson, Parisa Kordjamshidi, and Thomas E. Langan. "Deep convolutional neural network for flood extent mapping using unmanned aerial vehicles data." *Sensors* 19, no. 7 (2019): 1486.

Gebrehiwot, A.A., Hashemi-Beni, L., 2021. Three-Dimensional Inundation Mapping Using UAV Image Segmentation and Digital Surface Model. IJGI 10, 144. https://doi.org/10.3390/ijgi10030144

Gebrehiwot, A. A., Hashemi-Beni, L. (2022). 3D Inundation Mapping: A Comparison Between Deep Learning Image Classification and Geomorphic Flood Index Approaches. *Frontiers in Remote Sensing*, 3, 868104.

Guo, Z., Moosavi, V., Leitão, J.P., 2022. Data-driven rapid flood prediction mapping with catchment generalizability. Journal of Hydrology 609, 127726. https://doi.org/10.1016/j.jhydrol.2022.127726

Guo, Z., P. Leitao, J., Simoes E., N., Moosavi, V., 2020. Data-driven flood emulation Speeding up urban flood predictions by deep.pdf.

Hashemi-Beni, L., Gebrehiwot, A.A., 2021. Flood Extent Mapping: An Integrated Method Using Deep Learning and Region Growing Using UAV Optical Data. IEEE J. Sel. Top. Appl. Earth Observations Remote Sensing 14, 2127–2135. https://doi.org/10.1109/JSTARS.2021.3051873

Hashemi-Beni, Leila, Megha Puthenparampil, and Ali Jamali. "A low-cost IoT-based deep learning method of water gauge measurement for flood monitoring." *Geomatics, Natural Hazards and Risk* 15, no. 1 (2024): 2364777.

Iervolino, P., Guida, R., Iodice, A., Riccio, D., 2015. Flooding Water Depth Estimation With High-Resolution SAR. IEEE Trans. Geosci. Remote Sensing 53, 2295–2307. https://doi.org/10.1109/TGRS.2014.2358501

Kabir, S., Wood, D., Waller, S., 2023. A Deep Learning Model for Generalized Surface Water Flooding across Multiple Return Periods, in: ITISE 2023. Presented at the ITISE 2023, MDPI, p. 94. https://doi.org/10.3390/engproc2023039094

Liu, W.-C., Huang, W.-C., 2024. Evaluation of deep learning computer vision for water level measurements in rivers. Heliyon 10, e25989. https://doi.org/10.1016/j.heliyon.2024.e25989

Moy De Vitry, M., Kramer, S., Wegner, J.D., Leitão, J.P., 2019. Scalable flood level trend monitoring with surveillance cameras using a deep convolutional neural network. Hydrol. Earth Syst. Sci. 23, 4621–4634. https://doi.org/10.5194/hess-23-4621-2019

Muhadi, N.A., Abdullah, A.F., Bejo, S.K., Mahadi, M.R., Mijic, A., Vojinovic, Z., 2024. Deep learning and LiDAR integration for surveillance camera-based river water level monitoring in flood applications. Nat Hazards 120, 8367–8390. https://doi.org/10.1007/s11069-024-06503-6

Museru, M.L., Nazari, R., Giglou, A.N., Opare, K., Karimi, M., 2024. Advancing flood damage modeling for coastal Alabama residential properties: A multivariable machine learning approach. Science of The Total Environment 907, 167872. https://doi.org/10.1016/j.scitotenv.2023.167872

Popandopulo, G., Illarionova, S., Shadrin, D., Evteeva, K., Sotiriadi, N., Burnaev, E., 2023. Flood Extent and Volume Estimation Using Remote Sensing Data. Remote Sensing 15, 4463. https://doi.org/10.3390/rs15184463

Ronneberger, O., Fischer, P., Brox, T., 2015. U-Net: Convolutional Networks for Biomedical Image Segmentation, in: Navab, N., Hornegger, J., Wells, W.M., Frangi, A.F. (Eds.), Medical Image Computing and Computer-Assisted Intervention – MICCAI 2015, Lecture Notes in Computer Science. Springer International Publishing, Cham, pp. 234–241. https://doi.org/10.1007/978-3-319-24574-4_28

Schumann, G., Hostache, R., Puech, C., Hoffmann, L., Matgen, P., Pappenberger, F., Pfister, L., 2007. High-Resolution 3-D Flood Information From Radar Imagery for Flood Hazard Management. IEEE Trans. Geosci. Remote Sensing 45, 1715–1725. https://doi.org/10.1109/TGRS.2006.888103

Scorzini, A.R., Radice, A., Molinari, D., 2018. A New Tool to Estimate Inundation Depths by Spatial Interpolation (RAPIDE): Design, Application and Impact on Quantitative Assessment of Flood Damages. Water 10, 1805. https://doi.org/10.3390/w10121805

Shahabi, A., Tahvildari, N., 2024. A deep-learning model for rapid spatiotemporal prediction of coastal water levels. Coastal Engineering 190, 104504. https://doi.org/10.1016/j.coastaleng.2024.104504

Song, Z., Tuo, Y., 2021. Automated Flood Depth Estimates from Online Traffic Sign Images: Explorations of a Convolutional Neural Network-Based Method. Sensors 21, 5614. https://doi.org/10.3390/s21165614

Surampudi, S., Kumar, V., 2023. Flood Depth Estimation in Agricultural Lands From L and C-Band Synthetic Aperture Radar Images and Digital Elevation Model. IEEE Access 11, 3241–3256. https://doi.org/10.1109/ACCESS.2023.3234742

Wang, Y., Fang, Z., Hong, H., Peng, L., 2020. Flood susceptibility mapping using convolutional neural network frameworks. Journal of Hydrology 582, 124482. https://doi.org/10.1016/j.jhydrol.2019.124482

Wienhold, K.J., Li, D., Li, W., Fang, Z.N., 2023. Flood Inundation and Depth Mapping Using Unmanned Aerial Vehicles Combined with High-Resolution Multispectral Imagery. Hydrology 10, 158. https://doi.org/10.3390/hydrology10080158

World Bank, 2023. Urban population (% of total population) - United States [WWW Document]. World Bank Group. URL https://data.worldbank.org/indicator/SP.URB.TOTL.IN.ZS?locations=US (accessed 10.30.24).

Yokoya, N., Yamanoi, K., He, W., Baier, G., Adriano, B., Miura, H., Oishi, S., 2022. Breaking Limits of Remote Sensing by Deep Learning From Simulated Data for Flood and Debris-Flow Mapping. IEEE Trans. Geosci. Remote Sensing 60, 1–15. https://doi.org/10.1109/TGRS.2020.3035469